# Stochastic instability of a nonlinear oscillator

Alexander B. Rechester
*Bell Laboratories, Murray Hill, New Jersey 07974*

Thomas H. Stix*
*Department of Nuclear Physics, Weizmann Institute of Science, Rehovot, Israel*
(Received 11 October 1978)

The equation describing perturbed motion of a nonlinear oscillator is studied by a Hamiltonian formalism and by computer mapping. Other physical situations, including the motion of a charged particle in the field of two plane waves, the destruction of magnetic surfaces in a tokamak, and the bounce motion of a charged particle trapped in a magnetic field, can be described by the same equation. Theory predicts the regions of stochastic instability of orbits in a good agreement with computer calculations.

## I. INTRODUCTION

The purpose of this paper is to explore the conditions under which the solutions of

$$d^2x/dt^2 = -\sin x - \epsilon\lambda \sin(\lambda x - \Omega t)\,, \tag{1}$$

become unstable. Equation (1), which is in dimensionless form, can be used directly to describe a number of problems important in plasma physics: the motion of a charged particle in the field of two electrostatic plane waves,[1,2] the destruction of magnetic surfaces in a tokamak by resonant magnetic perturbations,[3] and the bounce motion of a charged particle trapped in a toroidal magnetic field but perturbed by a superposed electrostatic wave.[4] Moreover, Eq. (1) provides a simple model for processes which are described in full by more complicated equations, such as the cyclotron and cyclotron-harmonic acceleration of charged particles in a strong background magnetic field.[5-7]

The Hamiltonian for Eq. (1) is given by

$$H = H_0 + \epsilon H_1\,, \tag{2}$$

$$H_0 = \tfrac{1}{2}(dx/dt)^2 - \cos x\,, \tag{3}$$

$$H_1 = -\cos(\lambda x - \Omega t)\,. \tag{4}$$

With no loss of generality we can take $\lambda > 0$. We will consider the second term in Eq. (2) a perturbation, assuming $\epsilon \ll 1$. The unperturbed Hamiltonian (3) corresponds to the motion of a simple pendulum, and its trajectories projected on phase space $x, v = dx/dt$ lie on the lines of constant energy, $H_0 = \text{const}$ (Fig. 1). The separatrix, $H_0 = 1$, separates the closed or trapped trajectories from the untrapped.

When the perturbation is present, the Hamiltonian becomes time dependent, and energy is not conserved. There is, in this case, no longer any simple invariant of the motion for Eq. (1); nevertheless, when $\epsilon$ is small enough, the trajectories of Eq. (1) behave as if there were still such an invariant. A rigorous proof of the existence of exact invariants for the case of a periodic perturbation is given by the Kolmogorov-Arnold-Moser theorem (KAM),[8] which constructs convergent series that represent analytically such invariants when they do exist. A geometrical interpretation of the KAM theorem has also been given: plot the orbits in the space with coordinates $x$ modulo$2\pi$, $v = dx/dt$, and $\tau = \Omega t$ modulo$2\pi$, and visualize the unperturbed trajectories which now lie on toroidal surfaces. The intersection of these surfaces with the plane $\tau = \text{const}$ will appear as in Fig. 1. According to the KAM theorem, small perturbations do not destroy most of these invariant tori but only deform them slightly. The amazing stability of the invariant surfaces to perturbation persists up to a certain magnitude of perturbation. When the perturbation is big enough, almost all of the invariant surfaces will be destroyed in a certain region of the phase space, and most of the tra-

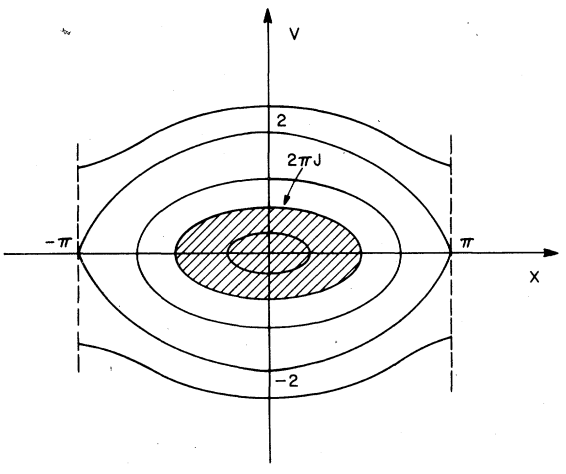


FIG. 1. Trajectories of unperturbed motion in phase space.

 

jectories in this region will wander about within the volume limited by the closest undestroyed surfaces. The property of motion in this case has been studied in ergodic theory,[8,9] and it has been shown that there is an instability which manifests itself in the exponential divergence of any two arbitrarily close trajectories. This behavior is called stochastic instability,[9] and we will be calculating where in phase space and for what range of parameters this instability exists.

Section II is devoted to analytic study. It is based on perturbation theory for $\epsilon \ll 1$ and on the resonance overlapping criterion.[10] This approach was first applied to Eq. (1) by Zaslavskii and Filonenko, studying motion primarily near the separatrix. We have also considered regions away from the separatrix, a wider range of parameters, and have found number of new results. In Sec. III we study Eq. (1) numerically by computer mapping, and this section serves to illustrate the analytic theory. Our results are summarized in Sec. IV.

## II. HAMILTONIAN PERTURBATION THEORY

The basic idea of our calculation is that destruction of an invariant is due to that component of a perturbation which resonates with the unperturned motion. To find these resonances it is very useful to introduce the action-angle variables $J$ and $\phi$ associated with the unperturbed Hamiltonian (3). Consider first the motion inside the separatrix. Equation (1) can be written

$$\frac{dJ}{dt} = -\epsilon \frac{\partial H_1}{\partial \phi}, \quad \frac{d\phi}{dt} = \omega(J) + \epsilon \frac{\partial H_1}{\partial J}, \tag{5}$$

$$\omega(J) = \frac{dH_0}{dJ}, \tag{6}$$

and the equations for the canonical transformation to new variables can be written

$$J = \frac{1}{2\pi} \oint dv\, dx, \tag{7}$$

$$S(x,J) = \int^x v(x,J)dx, \tag{8}$$

$$\phi = \frac{\partial S}{\partial J}. \tag{9}$$

In (7), the integral is taken over the area inside the closed trajectory in the phase space (Fig. 1); the Hamiltonian does not change, because the generating function $S$ is independent of time. It is, of course, the property that the frequency $\omega(J)$ is constant on the unperturbed orbits ($J = \text{const}$) that makes the action-angle variables especially convenient. The variable $\phi$ is periodic, with period $2\pi$. We now expand $H_1$ in a Fourier series in the angle variable $\phi$:

$$H_1 = \sum_{m,n} V_{mn}(J) e^{i(m\phi - n\Omega t)} + \text{c.c.}, \tag{10}$$

and note from (4) that $n$ takes on only the values $\pm 1$.

Consider now the special case where only one harmonic is nonzero in Eq. (10):

$$H_1 = 2|V_{mn}| \cos(w + w_0), \tag{11}$$

where $w = m\phi - n\Omega t$ and $w_0 = \arctan(\text{Re}\, V_{mn}/\text{Im}\, V_{mn})$. In this case there is an exact constant of motion

$$\psi(w,J) = \int [w(J) - (n/m)\Omega] dJ + \epsilon H_1(w,J), \tag{12}$$

and resonance occurs on that orbit, $J = J_{mn}$, which "sees" a constant phase of the perturbation, i.e., on which

$$dw/dt = m\omega(J_{mn}) - n\Omega = 0. \tag{13}$$

Expanding (12) in powers of $\Delta J = J - J_{mn}$ around the resonance, we get

$$\psi(w,J) \simeq \frac{1}{2} \frac{d\omega}{dJ} (\Delta J)^2 + 2\epsilon |V_{mn}| \cos(w + w_0) = \text{const}. \tag{14}$$

It may be observed that the contours of the invariant surfaces are those of islands, similar to Fig. 1 but with $v$ and $x$ replaced now by $J$ and $\phi$. The full width of the separatrix for these islands is

$$\Delta_{mn} = 4 \left| 2\epsilon V_{mn} \Big/ \frac{d\omega}{dJ} \right|^{1/2}_{J=J_{mn}}. \tag{15}$$

Equation (15) must be evaluated at $J = J_{mn}$.

If $H_1$ [Eq. (11)] contains two or more incommensurate harmonics, then there is no longer an exact constant of motion akin to $\psi(w,J)$ [Eq. (12)]. Stochastic instability developes whenever separatrices of neighboring islands overlap,[10] and we can parametrize the overlap condition by the quantity $s$,[9]

$$s = \tfrac{1}{2}(\Delta_{mn} + \Delta_{m'n'})/\Delta J_{mn}. \tag{16}$$

Here $m,n$ and $m',n'$ are mode numbers for neighboring resonances, $\Delta J_{mn} = |J_{m'n'} - J_{mn}|$. The overlap criterion says that most of the invariant tori will be destroyed for $s > 1$ in the region between islands[9,10] and describes well the stochastic transition in the case $\Delta_{mn} \approx \Delta_{m'n'}, m \sim m'$. However, the actual structure of invariant surfaces in the transitional region $0.7 \leq s \leq 1.5$ can be quite complicated.[2]

Now consider the case where many resonant modes are present with $|m| \gg 1$. From (13), with $m' = m \pm 1$ and $n' = n = \pm 1$, we can approximate

$$\Delta J_{mn} = \left| \frac{\omega^2}{\Omega} \frac{dJ}{d\omega} \right|_{J=J_{mn}} . \tag{17}$$

Then, using Eqs. (15)–(17), we can easily find

$$s^2 = 32 \frac{\Omega^2}{\omega^4} \left| \epsilon V_{mn} \frac{d\omega}{dJ} \right|_{J=J_{mn}} > 1 . \tag{18}$$

Inequality (18) can be used to determine instability regions.

Further analysis requires use of the specific Hamiltonian given in Eqs. (2)–(4). Carrying out the operations indicated in Eqs. (5)–(9) leads, for orbits inside the separatrix to[1,3]

$$0 \leq k^2 \equiv \tfrac{1}{2}(1+H_0) \leq 1, \quad J = (8/\pi)[E(k) - (1-k^2)K(k)] ,$$
$$x = 2 \sin^{-1}[k \, \mathrm{sn}(\alpha, k)], \quad v = 2k \, \mathrm{cn}(\alpha, k) , \tag{19}$$
$$S = 4[E(\mathrm{am}\alpha, k) - (1-k^2)\alpha], \quad \phi = \omega\alpha, \quad \omega = \pi/2K(k) .$$

In this set of relations, am, sn, and cn are Jacobian elliptic functions, $K$ is the complete elliptic integral of the first kind, $E(\phi, k)$ is the incomplete elliptic integral of the second kind, and $E(k) = E(\frac{1}{2}\pi, k)$. Some properties of these functions are presented in Appendix A. Using $k$ instead of $J$, we can write (18) in the form

$$s^2 = \frac{2J(k)}{k^2(1-k^2)\omega(k)} \Omega^2 |\epsilon V_{mn}|_{m\omega = n\Omega} > 1 , \tag{20}$$

where we have evaluated

$$\frac{d\omega}{dJ} = -\frac{1}{16} \frac{\omega^3 J}{k^2(1-k^2)} . \tag{21}$$

In order to use Eq. (20) we need the resonant value of $V_{mn}$, generally a quite complicated function of $\Omega$, $\lambda$, and $k$. We have calculated it analytically in Appendix B in different limits. For example, in the region $|\Omega| > \max(1, 2\lambda)$, the leading term of the asymptotic expansion is

$$|V_{mn}| = \omega \frac{|2\Omega|^{2\lambda - 1}}{\Gamma(2\lambda)} \exp[-|\Omega K'(k)|] , \tag{22}$$

Here $K'(k) = K(\sqrt{1-k^2})$, and we have used Eq. (B3) and resonance condition (13). Equation (22) shows that $V_{mn}$ is a rapidly varying function of $\Omega$ and $\lambda$, and modest changes in these parameters can alter dramatically the size of the stochastic region, given by Eq. (20), while the dependence on $\epsilon$ in (20) is just linear. Some numerical evaluations of Eqs. (20) and (22) are provided in Sec. II.

In the case $|\Omega| \ll 1$ the resonant condition (13) cannot be satisfied except very close to the separatrix. Near the separatrix $k \to 1$, $\omega(k) \approx \pi / \ln[8/(1-k)]$, so that $1 - k_{mn} = 8e^{-\pi |m/\Omega|}$. This case corresponds to a slow, adiabatic perturbation.

We note that $s^2$ in (20) goes to infinity as $k \to 1$, which indicates a region of instability near the separatrix. This region is very small when $|\Omega| \gg \max(1, 2\lambda)$ or $|\Omega| \ll 1$, and reaches its maximum size for $|\Omega| \sim \max(1, 2\lambda)$, when the phase velocity of the perturbation $\Omega/\lambda$ is of the order of the half-width of the primary island (see Fig. 1) in the case $\lambda \gtrsim 1$. For the case $\lambda \gg 1$ the stochastic region can occupy a considerable amount of trapped phase space (see Fig. 5), while for $\lambda \ll 1$ it is relatively small.

Consider now the case when resonance occurs near the bottom of the potential well, $k \ll 1$. It is then appropriate to expand (12) in powers of $J \to 0$, rather than $\Delta J \equiv J - J_{mn}$. Keeping the two first terms, we get

$$\psi = [1 - (n/m)\Omega]J - \tfrac{1}{16}J^2 + 2\epsilon v_{mn} J^{m/2} \cos(m\phi - n\Omega) , \tag{23}$$

where we have used $J \approx 2k^2$, $\omega \approx 1 - \frac{1}{8}J$, and $V_{mn} = v_{mn} J^{m/2}$ when $k \ll 1$ (see Appendices A and B). The perturbed surfaces around $k = 0$ can now be very different from the simple elliptic unperturbed surfaces. For example, when

$$m \simeq n\Omega \tag{24}$$

the first term in (23) may be neglected and, in the case of $1 \leq |m| \leq 4$, the unperturbed elliptic point, $k = 0$ becomes an unstable hyperbolic point. For the case $m = 4$ there is a threshold value of $|v_{4n}| \geq (32|\epsilon|)^{-1}$ at which this transformation takes place. In case of resonances with $m \geq 5$, the 0 point always preserves its identity. More generally, for $\Omega < m/n$, a chain of islands stretches out along the $J_{mn} = 16(1 - \Omega n/m)$ contour. However, as $\Omega$ approaches an integral value $m/n$, $1 \leq m \leq 4$, this island chain coalesces to a rosette pattern at $k = 0$, and the stable elliptic 0 point, $J = 0$, becomes an unstable hyperbolic point.

We turn now to examine motion outside the separatrix. In this case the phase-space trajectories of the unperturbed motion are not closed, but we can still introduce the convenient action-angle variables $J$ and $\phi$ for which the equations take forms (5) and (6). Instead of Eq. (7) we must now use

$$J = \frac{1}{2\pi} \int_0^{2\pi} v(x, H_0) dx . \tag{25}$$

Velocity $v$ is positive or negative depending on whether it describes motion above or below the separatrix. Owing to this ambiguity we have two sets of variables, $J_\pm$ and $\phi_\pm$. Using formulas (6), (8), (9), and (25), we can find[1,3]

$$J_\pm = \pm\frac{4}{\pi}kE(1/k), \quad k=\tfrac{1}{2}(1+H_0)\geq 1,$$
$$S_\pm = \pm 4kE\left(\frac{x}{2},\frac{1}{k}\right),$$
$$\phi_\pm = \phi = \frac{\pi\beta}{K(1/k)}, \quad x = 2\,\mathrm{am}(\beta,1/k), \tag{26}$$
$$v = \pm 2k\,\mathrm{dn}(\beta,1/k), \quad \omega_\pm = \pm\omega, \quad \omega = \frac{\pi k}{K(1/k)}.$$

The perturbation $H_1$ is not a periodic function of $\phi$ now, but its Fourier spectrum is still discrete, with $m=\lambda n+p$, $n=\pm 1$, and $p=0,\pm 1,\ldots$ (see Appendix C). Notice that $\lambda$ and $m$ can be nonintegers. The resonant condition (13) can now be written

$$m\omega_\pm = n\Omega. \tag{27}$$

Using the resonance overlapping criterion, we can derive the equation exactly as in (20) and (21), but with $J$, $\omega$, and $1-k^2$ being replaced by $J_\pm$, $\omega_\pm$, and $k^2-1$. In the region $|\Omega|>k\max(1,2\lambda)$ the leading term in the asymptotic expansion of $|V_{m,n}|$ is equal to

$$|V_{m,n}| = \tfrac{1}{2}(1+\mathrm{sgn}\Omega\omega_\pm)\omega\frac{|2\Omega|^{2\lambda-1}}{\Gamma(2\lambda)} \times \exp\left(-\left|\frac{\Omega K'(1/k)}{k}\right|\right). \tag{28}$$

Here we have used Eq. (C4) and resonance condition (27). It follows from this equation that resonances only appear above the separatrix when the phase velocity of the perturbation $\Omega/\lambda>0$ and below when $\Omega/\lambda<0$. When $2\lambda$ is an integer the factor arising from the signum function in Eq. (28) is present for all values of $\Omega$.

Close to the separatrix, $k\approx 1$, Eqs. (20), (22), and (28) are almost the same, the only difference being that $|J_\pm|$ outside is about two times smaller than $J$ inside, while $\omega$ is twice as big outside as it is inside. As a result the depth of the stochastic layer inside the separatrix is about twice its depth outside the separatrix.[3]

Finally, for resonances far away from the separatrix, $k\gg 1$, the resonant condition can be written

$$k_{mn} = \tfrac{1}{2}|\Omega/m|. \tag{29}$$

Corresponding Fourier coefficients have been calculated in Appendix C, yielding

$$V_{mn} = -\tfrac{1}{2}J_{|p|}(\lambda/4k_{mn}^2). \tag{30}$$

In the limit $k_{mn}^2\gg\frac{1}{4}\lambda$ all Fourier coefficients go to zero except $p=0$, with $V_{\lambda n,n}=-\frac{1}{2}$. This value corresponds to a perturbation in Eq. (4) which is itself considered an approximate resonance of the primary-island system.

## III. COMPUTER MAPPINGS

The practical way to determine for Eq. (1) whether invariant surfaces do or do not exist is to map trajectories in phase space $x, v=dx/dt$. Invariants exist if the points of a trajectory taken at successive times $t_p=2\pi p/\Omega, p=1,2,\ldots$, lie on a smooth curve. If the mapping is not a smooth curve but an irregular sequence of points which appear to fill a whole area, then we may say that the invariant surfaces are destroyed.

Equation (1) lends itself well to rapid computer integration, and the figures which accompany this paper were obtained by an extension of the method described in Ref. 2. Further details of the integration will be given elsewhere. In Figs. 2–6, the ordinate is $Y=v\lambda/\Omega$ and the abscissa is $x/2\pi$. Each plot is the superposition of $R$ runs; the number of mapping points in every run is equal to $N$. As initial conditions for these runs we took $x_0$, $Y_0+\delta Y_j$, where $\delta Y_j=(j-1)\delta Y$, $j=1,2,\ldots,R$.

Figure 2 is a detailed study of the case in which $\epsilon=\frac{1}{9}$, $\lambda=1$, and $\Omega=4$. The lines which appear solid on this picture are actually very dense mapping points ($N=800$). These lines correspond to the intersection of invariant surfaces with the plane of the picture. The scattered points belong to regions of stochastic instability. In order to check our theory, we have calculated in Table I the position, the island width, and the stochasticity parameter for the resonances inside and outside the separatrix, using Eqs. (13), (15), (20), (22), and (28). According to these calculations islands with $m=5,6$ and $n=1$ inside the separatrix, and $m=1,2,3$ and $n=1$ above the separatrix, do not overlap ($s<1$) and should be observable. We can discern most of these islands in Fig. 2, except $m=6,n=1$, which is close to the inside stochastic layer, and apparently none of our initial points lies close to the center of these islands. The $m=1,n=1$ island lies above $m=2,n=1$ and also cannot be seen for these initial data. We note in Fig. 2 that the upper stochastic layer above the separatrix is thick and has a wide transitional region with island structure, while the lower stochastic layer is comparatively thinner and is immediately bounded by an invariant curve.

Figure 3 is an example of the adiabatic ($\Omega\ll 1$) case, in which $\Omega=\frac{1}{16}$, $\lambda=1$, and $\epsilon=\frac{1}{16}$. In agreement with theory, there are no islands in this case even very close to the separatrix. But the mapping points do not lie on smooth curves either. Instead, they fill thin ring-shaped regions, owing to a very slow drift of action around its adiabatic value. We believe that this drift is due to high-order parametric effects (the frequency is a slowly changing function of time with period $2\pi/\Omega$),

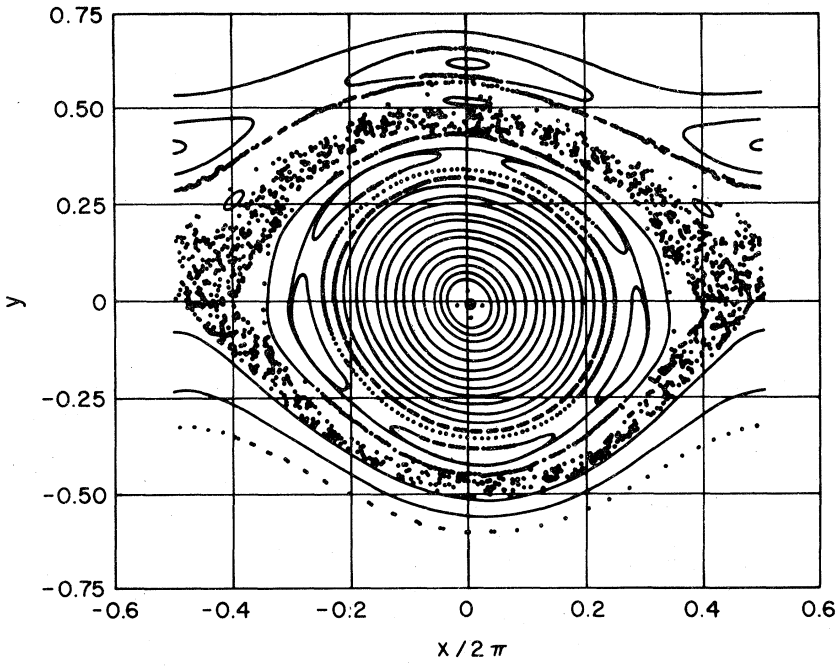


FIG. 2. Trajectories of perturbed motion for the case in which $\epsilon=\frac{1}{9}$, $\lambda=1$, $\Omega=4$, $R=30$, $N=800$, $x_0=0$, $Y_0=-0.6$, and $\delta Y=0.045$.

but a detailed discussion of this effect is beyond the scope of the present paper.

Figure 4 provides an interesting example of a case in which a stochastic region appears far away from the separatrix, while the motion near separatrix is quite stable. In this case $\Omega/\lambda=\frac{16}{3}\gg1$, and the stochastic layer near the separatrix should be exponentially small. Resonances above the separatrix have been calculated in Table II by means of Eqs. (18), (26), and (30). Overlapping ($s>1$) with $m=14$–$19$ is responsible for the stochasticity which is clearly observed on this figure. These resonances occur in the vicinity of $2k_m\approx|\Omega/\lambda|\approx|v|$ ($Y\approx1$). The harmonic $m=\lambda=16$ corresponds to $p=0$ in Eq. (30) and, because $k_{16}^2>\frac{1}{4}\lambda=4$, $|V_{16}|$ is close to its asymptotic value of 0.5.

Figure 5 corresponds to $\epsilon=\frac{1}{64}$, $\lambda=\Omega=32$, and was produced by mapping only one trajectory. The stochastic region occupies a considerable part of the phase space in this case, but stochasticity appears only above the original separatrix, in

TABLE I. Parameters pertinent to Fig. 2.

| $m$ | $k_{mn}$ | $J_{mn}$ | $\lvert V_{mn}\rvert$ | $\Delta_{mn}$ | $s$ |
|---|---|---|---|---|---|
| 5 | 0.783 | 1.35 | 0.005 41 | 0.325 | 0.37 |
| 6 | 0.916 | 1.97 | 0.007 54 | 0.315 | 0.76 |
| 7 | 0.965 | 2.26 | 0.007 62 | 0.258 | 1.3 |
| 8 | 0.984 | 2.4 | 0.007 11 | 0.201 | 2.0 |
| 9 | 0.993 | 2.48 | 0.006 5 | 0.152 | 3.1 |
| 10 | 0.997 | 2.51 | 0.005 92 | 0.114 | 4.6 |
| 11 | 0.999 | 2.53 | 0.005 41 | 0.085 | 6.9 |
| 12 | 0.999 | 2.54 | 0.004 97 | 0.062 | 10.2 |
| 13 | 1 | 2.54 | 0.004 59 | 0.046 | 15.1 |
| 14 | 1 | 2.54 | 0.004 27 | 0.033 | 22.4 |
| 7 | 1 | 1.27 | 0.008 54 | 0.023 | 15.9 |
| 6 | 1 | 1.28 | 0.009 98 | 0.044 | 7.3 |
| 5 | 1 | 1.29 | 0.012 1 | 0.080 | 3.33 |
| 4 | 1.01 | 1.34 | 0.015 6 | 0.141 | 1.58 |
| 3 | 1.06 | 1.51 | 0.024 2 | 0.239 | 0.81 |
| 2 | 1.26 | 2.06 | 0.060 6 | 0.443 | 0.487 |
| 1 | 2.13 | 4.01 | 0.5 | 1.33 | 0.33 |

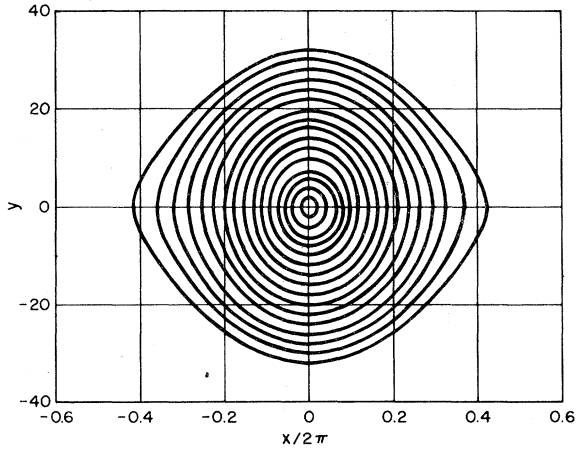


FIG. 3. Trajectories of perturbed motion for the case in which $\epsilon=\frac{1}{16}$, $\lambda=1$, $\Omega=\frac{1}{16}$, $R=16$, $N=1300$, $x_0=0$, $Y_0=2$, and $\delta Y=2$.

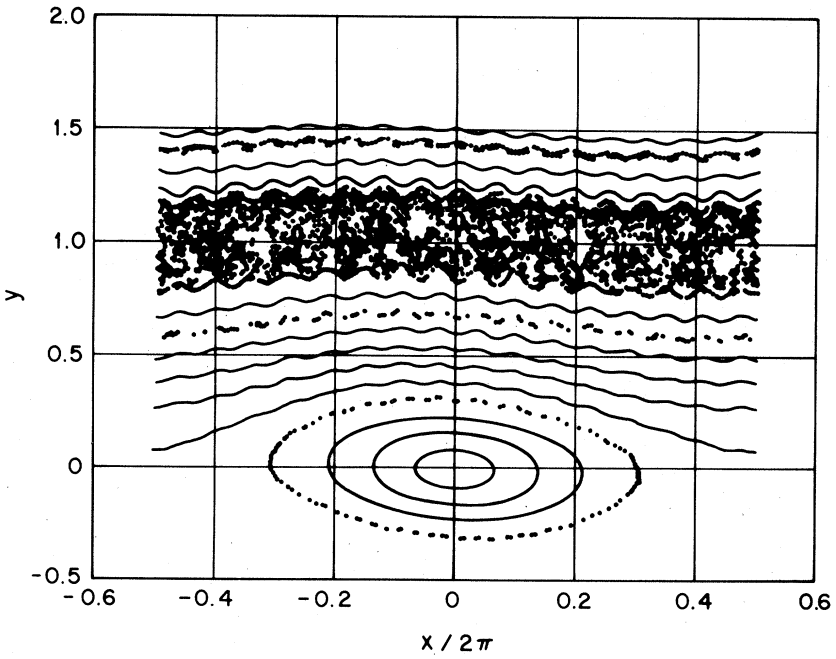


FIG. 4. Trajectories of perturbed motion for the case in which $\epsilon = \frac{1}{9}$, $\lambda = 16$, $\Omega = 85.3$, $R = 21$, $N = 1000$, $x_0 = 0$, $Y_0 = 0$, and $\delta Y = 0.3$.

agreement with the discussion following Eq. (28).

Figure 6 and 7 were run to illustrate the conversion of the stable elliptic point at $J = k = 0$ to an unstable hyperbolic point. The values of $\Omega = 2$ and $\Omega = 3$ lead, as expected, to $m = 2$ and $m = 3$ rosettes at the origin.

## IV. CONCLUSION

Our study has shown that formula (20) gives a good quantitative description of the regions of stochastic instability for Eq. (1) except very close to the bottom of potential well. Calculation of the Fourier coefficients $V_{mn}$ in Eq. (20) shows them to be very sensitive functions of $\lambda$ and $\Omega$. Even modest changes in these two parameters can yield dramatic modification of the stochasticity, while the dependence of $s^2$ on $\epsilon$ is just linear. We have also found that stochasticity appears above the upper separatrix or below the lower separatrix for $\Omega/\lambda > 0$ or $\Omega/\lambda < 0$, respectively. Moreover, we have found cases where stochastic instability appears away from the original separatrix while the motion near the separatrix is quite stable. Finally, we have found that the stable elliptic point at $J = 0$ can become an unstable hyperbolic if the resonant condition $|m| = |\Omega| \leq 4$ is satisfied. For $|m| \geq 5$, the 0 point remains stable.

TABLE II. Parameters pertinent to Fig. 4.

| $m$ | $k_{mn}$ | $J_{mn}$ | $\lvert v_{mn}\rvert$ | $\Delta_{mn}$ | $s$ |
|---|---|---|---|---|---|
| 24 | 1.92 | 3.57 | 8.94$E$-8 | 0.001 68 | 0.0115 |
| 23 | 1.99 | 3.72 | 7.94$E$-7 | 0.005 02 | 0.0314 |
| 22 | 2.07 | 3.89 | 6.95$E$-6 | 0.014 9 | 0.0849 |
| 21 | 2.16 | 4.07 | 5.94$E$-5 | 0.043 5 | 0.226 |
| 20 | 2.25 | 4.27 | 4.88$E$-4 | 0.125 | 0.587 |
| 19 | 2.36 | 4.50 | 0.003 75 | 0.346 | 1.47 |
| 18 | 2.48 | 4.75 | 0.025 6 | 0.904 | 3.44 |
| 17 | 2.61 | 5.02 | 0.141 | 2.12 | 7.19 |
| 16 | 2.76 | 5.34 | 0.466 | 3.86 | 11.6 |
| 15 | 2.93 | 5.69 | 0.113 | 1.9 | 5.02 |
| 14 | 3.13 | 6.1 | 0.010 3 | 0.573 | 1.32 |
| 13 | 3.36 | 6.57 | 4.61$E$-4 | 0.121 | 0.241 |
| 12 | 3.63 | 7.11 | 1.11$E$-5 | 0.018 8 | 0.0318 |

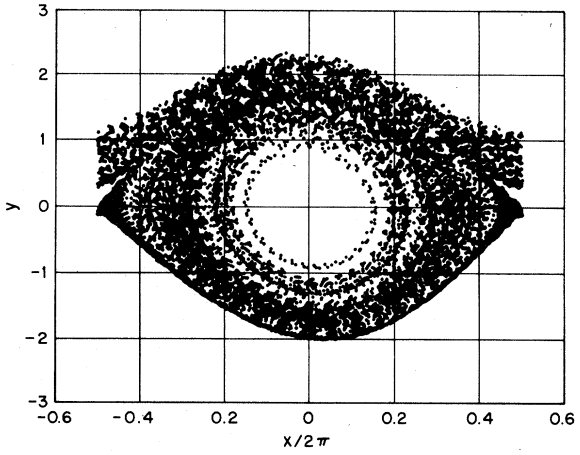


FIG. 5. Trajectories of perturbed motion for the case in which $\epsilon = \frac{1}{64}$, $\lambda = 32$, $\Omega = 32$, $R = 1$, $N = 10\,000$, $x_0 = 0$, $Y_0 = 1$, and $\delta Y = 0$.

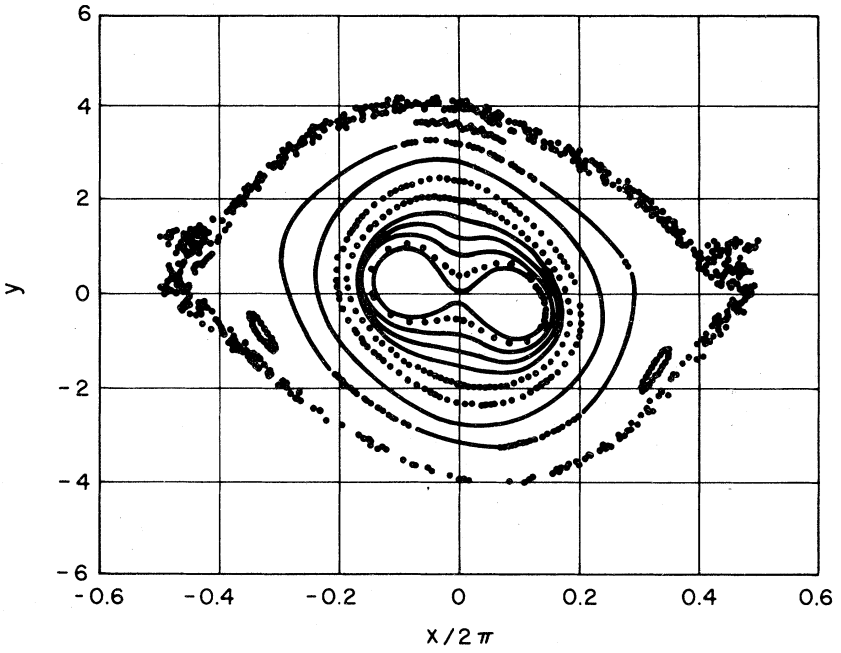


FIG. 6. Trajectories of perturbed motion for the case in which $\epsilon = \frac{1}{64}$, $\lambda = 4$, $\Omega = 2$, $R = 11$, $N = 700$, $x_0 = 0$, $Y_0 = 0.01$, and $\delta Y = 0.398$.

ACKNOWLEDGMENTS

A. B. Rechester benefited from discussions with Professor J. Ford and Dr. A. Hasegawa. T. H. Stix wishes to express his sincere appreciation to the members of the Department of Nuclear Physics of the Weizmann Institute of Science for their friendship and hospitality during his stay in Rehovot. A portion of this work was performed at the Plasma Physics Laboratory, Princeton, N.J. under USERDA Contract No. EY-76-C-02-3073.

## APPENDIX A

We list here some properties of elliptic integrals and of the Jacobi elliptic functions:

$k = 0$: $K(0) = E(0) = \frac{1}{2}\pi$, $\mathrm{sn}(u, 0) = \sin u$,

$k \ll 1$: $K'(k) \equiv K[(1 - k^2)^{1/2}] \simeq \ln(4/k)$,

$k = 1$: $E(1) = 1$, $K'(1) = \frac{1}{2}\pi$, $\mathrm{sn}(u, 1) = \tanh u$,

$k \simeq 1$: $K(k) \simeq \frac{1}{2} \ln[8/(1 - k)]$.

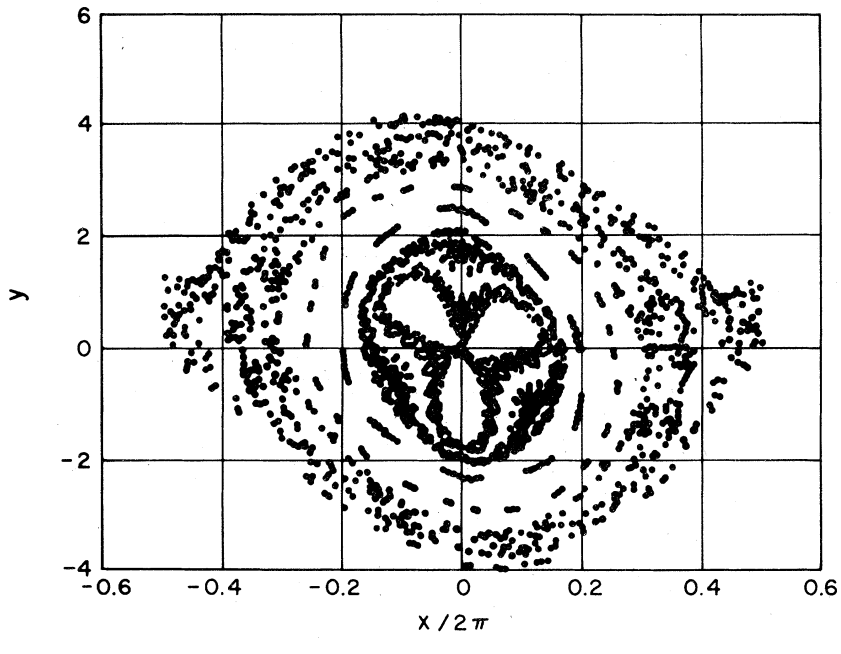


FIG. 7. Trajectories of perturbed motion for the case in which $\epsilon = \frac{1}{64}$, $\lambda = 6$, $\Omega = 3$, $R = 11$, $N = 300$, $x_0 = 0$, $Y_0 = 0.2$, and $\delta Y = 0.38$.

TABLE III. Periods, zeros, poles, and residues of Jacobi's elliptic functions ($m$ and $n$ are integers).

| Function | Primitive periods | Zeros | Poles | Residues |
|---|---|---|---|---|
| $\mathrm{sn}(u,k)$ | $4K,\ 2iK'$ | $2mK+2niK'$ | $2mK+(2n+1)iK'$ | $(-1)^m/k$ |
| $\mathrm{cn}(u,k)$ | $4K,\ 2K+2iK'$ | $(2m+1)K+2niK'$ | $2mK+(2n+1)iK'$ | $(-1)^{m+n}/ik$ |
| $\mathrm{dn}(u,k)$ | $2K,\ 4iK'$ | $(2m+1)K+(2n+1)iK'$ | $2mK+(2n+1)iK'$ | $(-1)^{n+1}i$ |

$$\frac{dK(k)}{dk}=\frac{E(k)}{k(1-k^2)}-\frac{K(k)}{k},\qquad \frac{\partial E(x,k)}{\partial k}=\frac{E-F}{k}.$$

## APPENDIX B

The Fourier coefficients $V_{mn}$ inside the separatrix, $0\leq k\leq 1$, are given by

$$V_{mn}=\frac{\Omega}{(2\pi)^2}\int_0^{2\pi}\int_0^{2\pi/\Omega}H_1(\phi,t)e^{-i(m\phi-n\Omega t)}\,d\phi\,dt, \tag{B1}$$

where

$$H_1=-\cos(\lambda x-\Omega t),\quad x=2\sin^{-1}(k\,\mathrm{sn}\alpha),\quad \alpha=\phi/\omega.$$

Carrying out the integration in time shows that $n$ is restricted to the values $\pm 1$. Then, expanding

$$\exp[in(\sin^{-1}k\,\mathrm{sn}\alpha)]=\mathrm{dn}\alpha+ink\,\mathrm{sn}\alpha,$$

we obtain

$$V_{mn}=-\frac{\omega}{4\pi}\int_0^{4K}d\alpha\,\exp(-im\omega\alpha)(\mathrm{dn}\alpha+ink\,\mathrm{sn}\alpha)^{2\lambda}. \tag{B2}$$

We first consider $m>0$ and depress the contour for this integral from the real axis to the lower half plane of the complex $\alpha$ plane, as illustrated in Fig. 8. Branch points of the integrand occur at $\alpha_1=-iK'$ and $\alpha_2=-iK'+2K$. If $2\lambda$ is an integer, then $\alpha_1$ and $\alpha_2$ are poles or zeros, depending on $n$, but our calculations will apply in this case too. Because the integrand is periodic with period $4K(k)$, the contributions along contours $C_3$ and $C_4$ cancel each other. Integrals along $C_5$ can be neglected because the exponent is negative and large when $m\gg 1$. The main contribution comes from integration along the branch cuts, and for this reason we use only the leading singular terms in the expansion of $\mathrm{dn}\alpha$ and $\mathrm{sn}\alpha$ near their poles (cf Table III). Making use of Hankel's formula for the gamma function, for $x>0$

$$\frac{2\pi i}{\Gamma(x)}=\int_C dz\,e^{-z}(-z)^{-x},$$

the contour of integration of which is shown in Fig. 9, we can finally find

$$V_{m,n}=-(\mathrm{sgn}mn)^{|m|}\omega\frac{(2\omega|m|)^{2\lambda-1}}{\Gamma(2\lambda)}e^{-\omega|m|K'}. \tag{B3}$$

The main contribution comes from $\alpha=\alpha_1$ when $n=1$, and from $\alpha\equiv\alpha_2$ when $n=-1$. We also included the case $m<0$ in Eq. (B3) by using the relation

$$V_{-m,-n}=V^*_{m,n}.$$

Equation (B3) is the leading term of the asymptotic expansion of $V_{m,n}$ in the region $\omega|m|>\max(1,2\lambda)$, as can be seen by considering $2\lambda$ an integer, in which case contribution from the poles can be calculated exactly. In the limit $k\ll 1$, $K(k)\to\frac{1}{2}\pi$, $K'(k)\to\ln(4/k)$, $\omega\to 1$, and (B3) can be further approximated

$$|V_{mn}|=\frac{(2|m|)^{2\lambda-1}}{\Gamma(2\lambda)}\left(\frac{k}{4}\right)^{|m|}, \tag{B4}$$

while for $\lambda\ll 1$, $\Gamma(2\lambda)\to 1/2\lambda$ and Eq. (B3) becomes

$$|V_{mn}|=(\lambda/|m|)e^{-\omega|m|K'}. \tag{B5}$$

Near the bottom of a potential well, $k\ll 1$, we can calculate $V_{m,n}$ with a small $m$ number, using

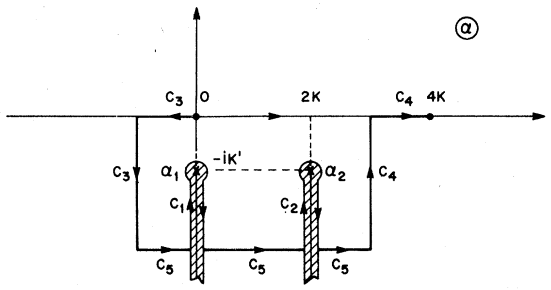


FIG. 8. Contour in the complex $\alpha$ plane for the integral in Eq. (B2).

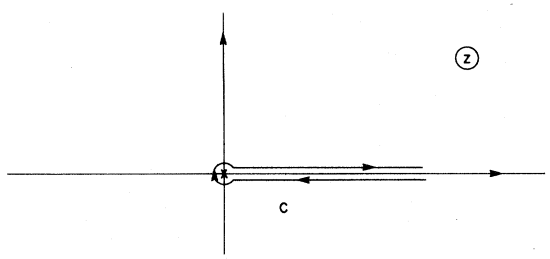


FIG. 9. Contour for the integration of Hankel's formula.

a different approximation for (B1). Expanding (B1) in powers of $k$, we have

$$x \approx 2k \sin\phi + O(k^2), \quad |V_{m,n}| = \tfrac{1}{2} J_{|m|}(2\lambda k). \tag{B6}$$

In this calculation we used the formula for Bessel functions with $m$ integral,

$$2\pi J_m(z) = \int_0^{2\pi} e^{iz\sin\phi - im\phi} d\phi. \tag{B7}$$

In the limit $\lambda k \ll 1$, (B6) can be approximated

$$|V_{m,n}| = |\lambda k|^{|m|}/2\Gamma(1+|m|). \tag{B8}$$

## APPENDIX C

In the region outside the separatrix the perturbation, expressed in action-angle variables for the unperturbed orbits, is, by (4) and (26),

$$H_1 = -\cos(2\lambda\ \mathrm{am}\beta - \Omega t), \quad \beta = K(1/k)\phi/\pi. \tag{C1}$$

Here $H_1$ is not a periodic function of $\phi$ as inside of the separatrix, and a Fourier integral in $\phi$ is appropriate. We expand

$$H_1 = \sum_{n=\pm 1} \int_{-\infty}^{\infty} V_{w,n} e^{i(w\phi - n\Omega t)} dw,$$

and invert

$$V_n(w) = \frac{\Omega}{(2\pi)^2} \int_{-\infty}^{\infty} \int_0^{2\pi/\Omega} H_1(\phi, t) e^{-i(w\phi - n\Omega t)} d\phi\, dt.$$

Taking the integral over time, we obtain

$$V_n(w) = -\frac{1}{4K(1/k)} \int_{-\infty}^{\infty} d\beta \exp(2in\lambda\ \mathrm{am}\beta - iw\pi\beta/K). \tag{C2}$$

We consider first case $w > 0$, and deform the contour of integration in the lower half plane as in Fig. 10. Here

$$\beta_p = -iK'(1/k) + 2pK(1/k), \quad p = 0, \pm 1, \ldots$$

are the singularities of the function

$$e^{i2n\lambda\,\mathrm{am}\beta} = (\mathrm{cn}\beta + in\ \mathrm{sn}\beta)^{2\lambda},$$

Generally, there are branch points, or poles if $2\lambda$ is integral. We can split the contour of integration $C$ into an infinite number of similar contours $C_p$ which are shifted a distance $2K$ to each other, and can then use the periodicity relation for function $\mathrm{am}\beta, p$ integral,

$$\mathrm{am}(\beta + 2pK) = \mathrm{am}\beta + \pi p,$$

together with the identity

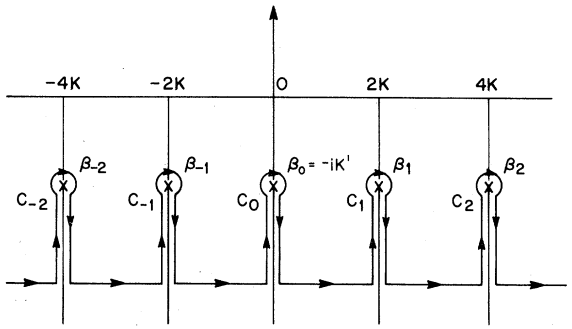


FIG. 10. Contour in the complex $\beta$ plane for the integral in Eq. (C2).

$$\sum_{p=-\infty}^{\infty} e^{-2\pi i p(w-\lambda n)} = \sum_{p=-\infty}^{\infty} \delta(w - \lambda n - p)$$

to obtain

$$V_n(w) = -\frac{1}{4K} \sum_{p=-\infty}^{\infty} \delta(w - \lambda n - p) \times \int_{C_0} d\beta \exp\left(\frac{-iw\pi\beta}{K(1/k)}\right) (\mathrm{cn}\beta + in\ \mathrm{sn}\beta)^{2\lambda}. \tag{C3}$$

The remaining calculations are very similar to those in Appendix B. The final result is

$$V_{m,n} = -(1 + \mathrm{sgn}mn)\omega \frac{(2\omega|m|)^{2\lambda-1}}{2\Gamma(2\lambda)} \times \exp\left(-\left|\frac{m\omega K'(1/k)}{k}\right|\right), \tag{C4}$$

$m = \lambda n + p, \quad p = 0, \pm 1, \ldots$ .

The spectrum is discrete even though $m$ is not an integer. Expression (C4) is the leading term of the asymptotic expansion in the region $\omega|m|/k > \max(1, 2\lambda)$. The factor arising from the signum function in Eq. (C4) is due to the fact that when $n$ changes from +1 to −1, poles of the function $\mathrm{cn}\beta + in\ \mathrm{sn}\beta$ become zeros and zeros become poles. Near the separatrix $k \approx 1$, Eqs. (B3) and (C4) are almost the same.

Far from the separatrix, a different approximation is useful. For $k \gg 1$, we can expand

$$x = 2\ \mathrm{am}(\beta, 1/k) \simeq 2\beta + (1/4k^2)\sin 2\beta + \ldots .$$

Using (C3), we can easily find Fourier coefficients with the small $m$ numbers:

$$|V_{m,n}| = \tfrac{1}{2} J_{|p|}(\lambda/4k^2), \quad m = \lambda n + p. \tag{C5}$$

---

*On leave from the Plasma Physics Laboratory, Princeton University, Princeton, N. J. 08540.

[1] G. M. Zaslavskii and N. N. Filonenko, Sov. Phys. JETP 27, 851 (1968).

[2] T. H. Stix, in *Proceedings of the Third Symposium on Plasma Heating in Toroidal Devices*, edited by F. Sindoni (Editrice Compositori, Bologna, 1976), p. 159.

[3] A. B. Rechester and T. H. Stix, Phys. Rev. Lett. 36,

587 (1976).
[4]G. R. Smith, Phys. Rev. Lett. 38, 970 (1977).
[5]G. R. Smith and A. N. Kaufman, Phys. Rev. Lett. 34, 1613 (1975), also Phys. Fluids 21, 2230 (1978).
[6]A. Fukuyama, H. Momota, R. Itatani, and T. Takizuka, Phys. Rev. Lett. 38, 701 (1977).
[7]C. F. F. Karney and A. Bers, Phys. Rev. Lett. 39, 550 (1977).
[8] Usually the KAM theorem is formulated for a conservative Hamiltonian system, but the reader can find the modification of this theorem for a periodic time-dependent perturbation, in V. I. Arnold , *Mathematical Methods in Classical Mechanics* (Nauka, Moscow, 1974), p. 376; V. I. Arnold and A. Avez, *Ergodic Problems of Classical Mechanics* (Benjamin, New York, 1968).
[9]G. M. Zaslavskii and B. V. Chirikov, Sov. Phys. Usp. 14, 549 (1972). B. V. Chirikov, At. Energy 6, 630 (1959) [J. Nucl. Energy C 1, 253 (1960)].
[10]M. N. Rosenbluth, R. Z. Sagdeev, J. B. Taylor, and G. N. Zaslavskii, Nucl. Fusion 6, 297 (1966).